

## Research Article

# Development of Thiazolidinone-Based Pyrazine Derivatives: Synthesis, Molecular Docking Simulation, and Bioevaluation for Anti-Alzheimer and Antibacterial Activities

Uzma Jehangir,<sup>1</sup> Shoaib Khan ,<sup>2</sup> Razaqat Hussain,<sup>3</sup> Yousaf Khan ,<sup>1</sup> Farhan Ali ,<sup>2</sup> Asma Sardar,<sup>3</sup> Samina Aslam,<sup>4</sup> and Mozhgan Afshari <sup>5</sup>

<sup>1</sup>Department of Chemistry, COMSATS University Islamabad Campus, Islamabad 45550, Pakistan

<sup>2</sup>Department of Chemistry, Abbottabad University of Science and Technology (AUST), Abbottabad, Pakistan

<sup>3</sup>Department of Chemistry, Hazara University, Mansehra 21120, Pakistan

<sup>4</sup>Department of Chemistry, Sardar Bahadur Khan Women's University, Quetta, Balochistan, Pakistan

<sup>5</sup>Department of Chemistry, Shoushtar Branch, Islamic Azad University, Shoushtar, Iran

Correspondence should be addressed to Shoaib Khan; [shoaibkhanswati@gmail.com](mailto:shoaibkhanswati@gmail.com) and Mozhgan Afshari; [mozhgan.afshari@iau.ac.ir](mailto:mozhgan.afshari@iau.ac.ir)

Received 9 September 2023; Revised 19 December 2023; Accepted 6 January 2024; Published 22 January 2024

Academic Editor: Mohd Sajid Ali

Copyright © 2024 Uzma Jehangir et al. This is an open access article distributed under the Creative Commons Attribution License, which permits unrestricted use, distribution, and reproduction in any medium, provided the original work is properly cited.

It is well recognized that heterocyclic compounds have exceptional biomedical applications, which has led scientists to become increasingly interested in their use in this field in the recent past. It is the aim of this study, using a multistep method based on thiazolidinone derivative synthesis, to synthesize thiazolidinone derivatives derived from pyrazine molecules (1–12). As a result of analyzing 1H-NMR, 13C-NMR, and HREI-MS data, the structures of these derivatives were determined. The minimum inhibitory concentration (MIC) of these drugs was also determined alongside the donepezil ( $IC_{50} = 10.10 \pm 0.10 \mu M$ ) to determine their potential as anti-Alzheimer agents. Among the screened derivatives, 1 ( $IC_{50} = 4.10 \pm 0.20 \mu M$ ), 2 ( $IC_{50} = 2.20 \pm 0.20 \mu M$ ), 4 ( $IC_{50} = 2.30 \pm 0.20 \mu M$ ), 5 ( $IC_{50} = 5.80 \pm 0.30 \mu M$ ), 6 ( $IC_{50} = 6.30 \pm 0.20 \mu M$ ), 8 ( $IC_{50} = 5.20 \pm 0.10 \mu M$ ), 9 ( $IC_{50} = 5.20 \pm 0.40 \mu M$ ), 10 ( $IC_{50} = 8.30 \pm 0.40 \mu M$ ), and 11 ( $IC_{50} = 8.10 \pm 0.70 \mu M$ ) showed potent activity. In addition, the synthesized moieties were screened against *E. coli* to determine whether there were any antimicrobial properties. It was found that most of the compounds were more potent inhibitors of bacterial growth in comparison to streptomycin, the reference drug. There have been several molecular docking experiments conducted to gain a deeper understanding of how these compounds interact with the active sites of enzymes to gain a greater understanding of their functional mechanisms.

## 1. Introduction

Alzheimer's disease primarily affects human brains, in which two enzymes, acetylcholinesterase (AChE) and butyrylcholinesterase (BuChE), play crucial roles. Several enzymes are responsible for hydrolyzing acetylcholine, resulting in choline and acetic acid [1]. This enzyme hydrolyzes acetylcholine, which plays an important role in many cognitive functions of the brain, and a deficit in its production leads to cognitive decline [2]. Alzheimer's disease is characterized as a persistent and chronic neurological

condition that causes ongoing disturbances in the brain's cholinergic system, leading to a diverse range of symptoms such as disorientation, cognitive impairment, challenges in problem solving, and memory decline [3–5]. The main objective in the endeavor to develop a treatment for Alzheimer's disease is to specifically target the enzymes AChE and BuChE [6, 7].

Acetylcholinesterase is primarily found in cholinergic neurons, muscle tissue, and the brain, whereas butyrylcholinesterase is predominantly located in the lungs, heart, liver, kidneys, and intestines [8–10]. The enzymatic activity

and physiological role of acetylcholinesterase (AChE), which is notably abundant in the brain, primarily include the hydrolysis of ester-containing compounds. When the functioning of acetylcholine decreases, the activity of BuChE increases. In instances of this kind, the use of powerful drugs remains imperative to alleviate enzyme activity [11]. Furthermore, it is worth noting that the Food and Drug Administration (FDA) has approved some pharmacological interventions aimed at treating Alzheimer's disease. These drugs include donepezil, rivastigmine, tacrine, and galantamine [12]. Nevertheless, the efficacy of these treatments is constrained, and their possible adverse effects, such as gastrointestinal pain and liver damage, emphasize the necessity for additional progress in the development of treatment alternatives [13–16].

Pyrazines (1,4-diazabenzene) are volatile chemical compounds having a monocyclic aromatic ring that have antibacterial characteristics [17, 18]. Pyrazine production occurs in both mammals and plants [19]. However, pyrazines are synthesized by a few bacterial species, including *Pseudomonas*, *Bacillus*, *Streptomyces*, and *Paenibacillus* [20–22]. Pyrazine has been found to exhibit therapeutic properties such as antithrombogenicity [23], antimicrobial activity, tuberculous activity [18, 24], and anticholinesterase [25] and also exhibited inhibition against thymidine phosphorylase [26]. Nature is hepatoprotective and rigorous. However, certain pyrazines are toxic, such as those that impede cytochrome P450 synthesis [27] or activate liver microsomal explode hydrolase, an enzyme used in mammalian detoxification [28, 29]. As pyrazine and thiazolidinone moieties are biologically active [30–40], herein the current work, N-containing derivatives such as pyrazine-based thiazolidinone derivatives were synthesized and tested for biological activity to analyze their substantial impacts on Alzheimer's disease. Furthermore, the inhibitory actions were investigated further using molecular docking investigations (Figure 1).

## 2. Materials and Methods

**2.1. General Information.** The chemicals and reagents utilized in this research were predominantly obtained from commercial sources, with a particular emphasis on Sigma-Aldrich, a reputable supplier based in the United States. Nuclear magnetic resonance (NMR) examinations were performed using an Advanced Bruker AM 600 MHz spectrometer. The experimental procedure involved the acquisition of high-resolution electron impact mass spectra utilizing a Finnegan MAT-311A mass spectrometer manufactured in Germany. The procedure encompassed performing thin layer chromatography (TLC) on aluminum plates coated in advance with silica gel (Kieselgel 60, 254, E. Merck, Germany). The chromatogram was visualized using UV light with wavelengths of 254 nm and 365 nm.

**2.2. General Procedure for the Synthesis of Pyrazine-Based Thiazolidinone Derivatives (1–12).** Thiazolidinone derivatives (1–12) based on pyrazine were synthesized through a series of three consecutive phases. In the beginning, an

equimolar amount of different substituted benzene isothiocyanates (1 mmol, 0.8 g) and 2-amino-5-chlorobenzaldehyde (1 mmol) (I) were mixed in 10 mL of ethanol, along with triethylamine (3–5 drops), resulting in the formation of a thiourea intermediate (II). The intermediate (1 mmol 0.6 g) (II) was subsequently cyclized by agitation for approximately 5 hours in a mixture including 1 equivalent of chloroacetic acid (1 mmol), 10 mL of glacial acetic acid, and sodium acetate as a catalyst, leading to the generation of the thiazolidinone substrate (III). The synthesis of pyrazine-based thiazolidinone derivatives (1–12) was achieved by combining 1 equivalent of thiazolidinone substrate (1 mmol 0.5 g) (III) with 1 equivalent of 5-chloropyrazin-2-amine in 10 mL of ethanol. The utilization of glacial acetic acid as a catalyst (12–15 drops) in this reaction led to the successful synthesis of the desired derivatives, achieving favorable yields.

**2.3. Assay Protocol for the Molecular Docking Study.** A molecular docking study was performed using the AutoDock Vina software tool to investigate the binding mechanisms of the synthesized compounds with the target enzyme, acetylcholinesterase (AChE). The outcomes of our investigation conformed to the conclusions obtained from both our laboratory experiments and computer simulations. Protein Data Bank crystal structures were used to perform the docking analysis. For AChE, we extracted the crystal structure using the PDB code 1ACL. Following that, we proceeded to enhance the enzyme and chemical structures by decreasing their energies via protonation, employing the default parameters of the MOE-Dock module. The revised enzyme and chemical structures were subsequently utilized for the subsequent docking analysis [41–49].

**2.4. Assay Protocol for Acetylcholinesterase Inhibition.** A previously utilized approach was implemented to evaluate the inhibition of acetylcholinesterase (AChE). To provide a concise overview of the procedure, stock solutions of the test analogs were produced by dissolving them in DMSO at a concentration of 1 mg/mL. Serial dilutions were performed to create working solutions within the concentration range of 1–100  $\mu\text{g/mL}$ . Dimethyl sulfoxide (DMSO) and water were blended to make the solutions. As a result of serial dilution, different solutions are progressively diluted, resulting in concentrations such as 0.1 mg/mL and 0.2 mg/mL.

Afterwards, various concentrations of the test compounds (10  $\mu\text{L}$ ) were combined with a solution containing sodium phosphate buffer (0.1 M; pH 8.0; 150  $\mu\text{L}$ ) and acetylcholinesterase (0.1 U/mL; 20  $\mu\text{L}$ ). This mixture was then allowed to preincubate for 15 minutes at a temperature of 25°C. The reaction was initiated by adding DTNB (1 mM; 10  $\mu\text{L}$ ) and AChEI (1 mM; 10  $\mu\text{L}$ ). The reaction mixture was thoroughly mixed using a cyclomixer and then incubated at 25°C for 10 minutes. Following this, the measurement of absorbance was conducted at a specific wavelength of 410 nm utilizing a microplate reader, where a blank reading was employed as the reference. The space was filled with 10  $\mu\text{L}$  of dimethyl sulfoxide (DMSO) instead of the experimental material. This solution consisted of 5% DMSO and 95% water.

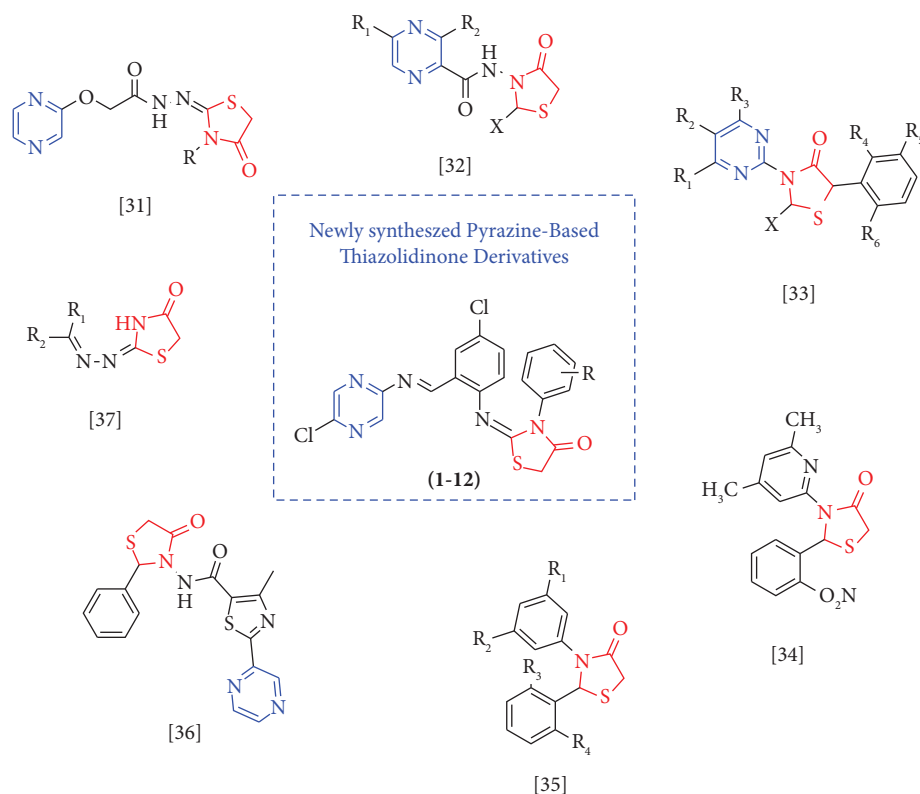


FIGURE 1: Rationale of the current study.

The calculation of the inhibition % was performed using the formula specified in equation X, where donepezil (0.01–100  $\mu\text{g/mL}$ ) was utilized as the positive control.

$$\% \text{ inhibition} = \frac{(\text{Absorbance of control} - \text{Absorbance of a compound})}{\text{Absorbance of control}} \times 100. \quad (1)$$

The  $\text{IC}_{50}$  value was determined by generating a nonlinear regression plot, which relates the percentages of inhibition to the concentration. GraphPad Prism software (version 5.3) was utilized for the analysis.

### 3. Results and Discussion

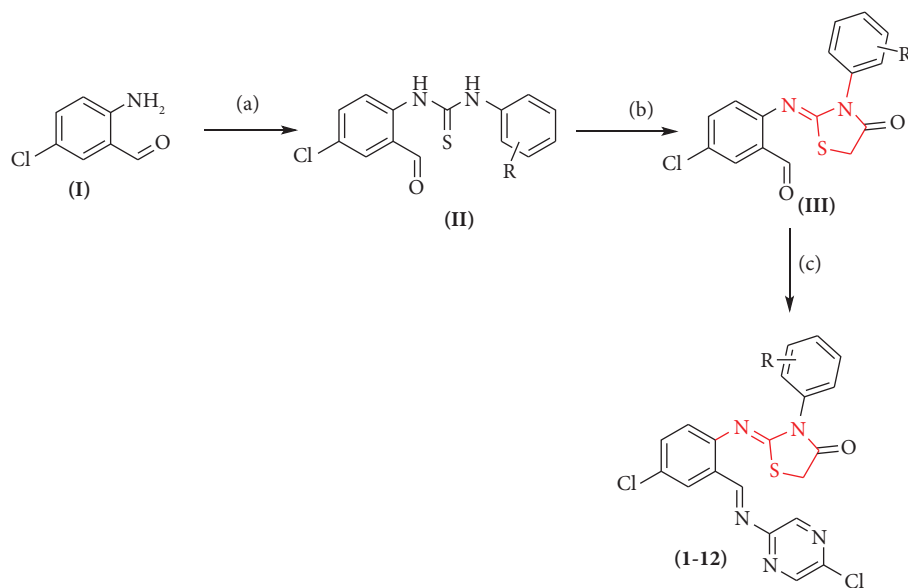
**3.1. Chemistry.** The synthetic procedure was initiated by the treatment of 2-amino-5-chlorobenzaldehyde (1 mmol 0.8 g) (I) with variously substituted phenyl isothiocyanates (1 mmol) in the presence of solvent ethanol. Triethylamine ( $\text{Et}_3\text{N}$ ) (3–5 drops) was introduced into the reaction mixture and refluxed the reaction mixture for 4 hours, resulting in the formation of thiourea derivatives (II). These aforementioned derivatives (II) (1 mmol) were then subjected to further refluxing with chloroacetic acid (1 mmol) in the presence of glacial acetic acid (10 ml) and sodium acetate for about 5 hours, yielding thiazolidinone derivatives (III).

In the final step, thiazolidinone substrate (1 mmol, 0.5 g) (III) was reacted with 5-chloropyrazin-2-amine in a solvent ethanol, in the presence of glacial acetic acid (10 mL), under

reflux conditions for approximately 3 hours. This step led to the synthesis of the targeted thiazolidinone-derived pyrazine-based Schiff base derivatives (1–12). The progress of the reaction was monitored with the help of TLC after every 45-minute interval during refluxing, and the resulting compounds were purified by washing with n-hexane.

Following the collecting process, the samples were subjected to additional characterization utilizing  $^1\text{H-NMR}$ ,  $^{13}\text{C-NMR}$ , and HREI-MS studies. These analytical techniques facilitated the identification of protons, carbons, and various functional groups present within the synthesized molecules, respectively (Scheme 1).

**3.2. Biological Profile.** The biochemical profiles describe the better biological potentials of the synthesized compounds against acetylcholinesterase (AChE) and *Escherichia coli* to investigate the antibacterial activity. A molecule's biological effects are strongly influenced by several factors, such as the type of atom, the number of atoms, and the configuration of substituents attached to an aromatic ring. The present study



SCHEME 1: Synthetic route for the synthesis of pyrazine-based thiazolidinone scaffolds (1-12): (a) different substituted phenylisothiocyanates, EtOH, Et<sub>3</sub>N, and reflux 4 hrs; (b) chloroacetic acid, acetic acid, sodium acetate, and reflux 5 hrs; and (c) 5-chloropyrazin-2-amine, acetic acid, ethanol, and reflux 3 hrs.

aims to synthesize and evaluate for their biological significance a series of substituted analogs that have been substituted with different molecules.

**3.2.1. Acetylcholinesterase Inhibitory Activity.** In order to determine the ability of synthetic compounds to inhibit acetylcholinesterase, the compounds were tested against donepezil, a standard prescription drug for acetylcholinesterase inhibition. Several compounds were found to have significant potential due to the presence of various substituents that have properties that allow them to form hydrogen bonds with the active sites of enzymes, which reduces the enzymatic activity of the enzyme. It was discovered that these scaffolds had better binding interactions in structure-activity relationships (SARs), in which the same substituted scaffolds were compared with standard drug profiles, as shown in the figures below, to determine which scaffolds had better binding interactions (Figure 2) [50].

**(1) Structure-Activity Relationship.** In the present studies, different substituted pyrazine-based thiazolidinone scaffolds were synthesized (1-12) by different reaction procedures (Scheme 1). Based on substituents, these scaffolds have been classified on the position of substituents, meaning the same substituents present varied positions on aromatic rings [51]. The biological significances of these compounds were investigated which depend upon the position, number, and nature of substituents (Table 1). The comparison criteria were set for trifluoro-substituted scaffolds (1, 2, and 4), showing that the most potent profile might be attributed to the presence of three fluorine atoms which make strong hydrogen bonding with the enzyme's active sites, therefore reported as the excellent acetylcholinesterase (AChE) inhibitors of the tested series along with minimum inhibitory

concentration (MIC) such as  $IC_{50} = 4.10 \pm 0.20$ ,  $2.20 \pm 0.20$ , and  $2.30 \pm 0.20 \mu M$ , respectively. The nitro group at the *ortho* position of these moieties also enhanced the inhibitory profile due to the presence of heteroatom such as nitrogen and oxygen, which are also involved in the formation of hydrogen bond through van der Waals interactions; this group also plays a significant role in the inhibitory profile of molecules; thus, these scaffolds (1, 2, and 4) showed many potentials compared to that of donepezil ( $IC_{50} = 10.10 \pm 0.10 \mu M$ ). The excellent potential among the trifluoro-substituted scaffolds was shown by analog 2; it might be the presence of the trifluoro group at the *para* position of the aromatic ring which strongly binds with the enzyme, thus considered as ranked-1 scaffold. A similar relationship of scaffolds (5 ( $IC_{50} = 5.80 \pm 0.30 \mu M$ ), 6 ( $IC_{50} = 6.30 \pm 0.20 \mu M$ ), and 8 ( $IC_{50} = 5.20 \pm 0.10 \mu M$ ) bearing two fluoro groups at varied positions on aromatic ring exhibited a significant biological profile. Among these scaffolds, the potent behavior was shown by analog 5; it might be the presence of the fluoro group at *para*- and *meta*-positions of the ring which increased the nucleophilicity in the ring to enhance the interactions, thus reducing the enzyme activity. The remaining two scaffolds (6 and 8) were also found with good potential in comparison to the reference drug because they also possess fluoro groups on varied positions such as two *meta*-positions (scaffold 6) and *ortho*- and *meta*-positions (scaffold 8). Similarly, scaffolds bearing the nitro group (9  $IC_{50} = 5.20 \pm 0.10 \mu M$ , 10  $IC_{50} = 8.30 \pm 0.40 \mu M$ , and 11  $IC_{50} = 8.10 \pm 0.70 \mu M$ ) also displayed few folds better potentials than donepezil. It may be the result of the presence of a nitro group which involves the hydrogen bond formation. The presence of a chloro group at different positions of the ring also enhances the nucleophilicity of the ring which might also engage the enzyme. A comparable profile was also found in the case of scaffold 3 ( $IC_{50} = 8.10 \pm 0.10 \mu M$ ) having groups such as

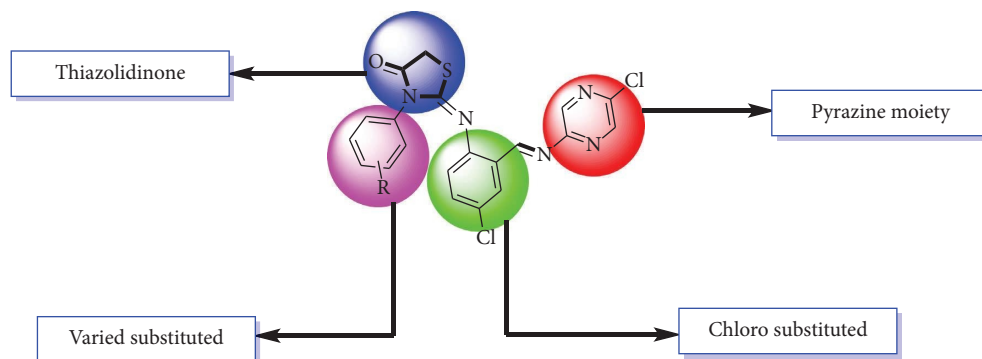


FIGURE 2: Representation of the general skeleton of synthesized moieties.

chloro and methyl at *meta*- and *para*-positions, respectively. Among the scaffolds investigated, 7 and 12 showed moderate to poor inhibitory potential. In comparison with the standard drug donepezil, these scaffolds showed decreased inhibitory effectiveness due to the presence of bulky groups. This resulted in reduced activity of these moieties.

**3.2.2. Antibacterial Profile.** We also looked at the antibacterial implications of all the compounds we made by testing them against *E. coli*. We found that the synthetic compounds had stronger inhibitory action than the gold standard antibiotic streptomycin, and we measured the compounds' zones of inhibition. The synthetic chemicals were also tested for their inhibitory efficacy against *E. coli* strains. There were maximal inhibitory concentrations (Max. inhibition % age) for the chosen scaffolds (1, 2, 4, 5, 6, 8, 9, 10, and 11). Due to the presence of distinct substituents at different places on the ring, it was further proved that these scaffolds displayed greater potential. This arrangement improved their performance while reducing any negative impacts. Figure 3 displays the inhibition percentages of various scaffolds. When compared to the standard medication streptomycin (37.5%), the other examined scaffolds had inhibition rates of 2, 3, 4, 5, 30, 1.1%, 6, 28.5%, 8, 30.3%, 9, 25.9%, 10, 25.2%, and 11, 28.8%, respectively. Analog 1 exhibited the highest inhibition rate among these scaffolds. The other scaffolds in the series that were tested showed very little promise, maybe because of the large groups that were linked to the aromatic ring [52].

**3.3. Molecular Docking Studies.** Pyrazine-based thiazolidinone derivatives (1–12) among better potentials shown by scaffolds (1, 2, 4, and 5) have been subjected to molecular docking studies to investigate the compounds' potential for interacting with the enzyme's active sites. Our research groups have also worked on a similar protocol of molecular docking which was performed, using different software such as the AutoDock tool (1.5.7), PyMol, and Discovery Studio visualizer [41–45]. The protein was obtained from a Protein Data Bank (PDB) with the PDB code 1Acl. Its protein-ligand interactions (PLIs) profile was explored in which receptor sites, type of bonding, and distance were calculated as shown in Table 2. The docking results showed the binding modalities in

terms of active sites both in protein and synthesized compounds which are represented in 2D and 3D structures for the subjected compounds as shown in Figures 4–7.

### 3.4. Experimental Analysis

**3.4.1. (E)-2-((4-Chloro-2-((E)-((5-chloropyrazin-2-yl)imino)methyl)phenyl)imino)-3-(2-nitro-5-(trifluoromethyl)phenyl)thiazolidin-4-one (1).** Yield, 63%; pale yellow solid,  $R_f$  value 0.52 (7:3 n-hex: EtOAc), m.p. 183–184°C;  $^1\text{H-NMR}$  (600 MHz, DMSO- $d_6$ ):  $\delta$  9.20 (s, 1H, N=CH), 8.86 (s, 1H, Cl-pyrazin-H), 8.68 (s, 1H, Cl-pyrazin-H), 8.42 (s, 1H, Ar-H), 8.36 (d,  $J$  = 8.4 Hz, 1H, Ar-H), 8.29 (s, 1H, Ar-H), 8.22 (d, 1H,  $J$  = 8.9 Hz, Ar-H), 8.14 (d,  $J$  = 8.4 Hz, 1H, Ar-H), 8.03 (d,  $J$  = 8.3 Hz, 1H, Ar-H), 3.59 (s, 2H, S-CH $_2$ );  $^{13}\text{C-NMR}$  (150 MHz, DMSO- $d_6$ ):  $\delta$  182.3, 167.1, 164.2, 160.5, 157.6, 155.3, 154.9, 153.4, 152.6, 150.7, 149.2, 149.7, 148.0, 148.1, 147.6, 134.8, 130.4, 129.0, 123.1, 115.2, 40.2; HREI-MS:  $m/z$  calculated for  $\text{C}_{21}\text{H}_{11}\text{Cl}_2\text{F}_3\text{N}_6\text{O}_3\text{S}$ ,  $[\text{M}]^+$  555.1357 Found 555.1348.

**3.4.2. (E)-2-((4-Chloro-2-((E)-((5-chloropyrazin-2-yl)imino)methyl)phenyl)imino)-3-(2-nitro-4-(trifluoromethyl)phenyl)thiazolidin-4-one (2).** Yield, 66%; white solid,  $R_f$  value 0.59 (7:3 n-hex: EtOAc) m.p. 199–200°C;  $^1\text{H-NMR}$  (600 MHz, DMSO- $d_6$ ):  $\delta$  9.19 (s, 1H, N=CH), 8.92 (s, 1H, Cl-pyrazin-H), 8.72 (s, 1H, Cl-pyrazin-H), 8.64 (s, Ar-H, 1H), 8.47 (d,  $J$  = 8.5 Hz, 1H, Ar-H), 8.42 (s, ArH, ArH, 1H), 8.37 (d, 1H,  $J$  = 8.0 Hz, Ar-H), 8.31 (d,  $J$  = 8.2 Hz, 1H, Ar-H), 8.13 (d,  $J$  = 8.3 Hz, 1H, Ar-H), 3.64 (s, 2H, S-CH $_2$ );  $^{13}\text{C-NMR}$  (150 MHz, DMSO- $d_6$ ):  $\delta$  184.9, 164.9, 163.3, 162.2, 157.8, 156.6, 155.4, 153.8, 152.6, 150.3, 149.9, 149.7, 148.2, 147.5, 147.0, 136.4, 132.3, 127.6, 123.7, 118.5, 43.01; HREI-MS:  $m/z$  calculated for  $\text{C}_{21}\text{H}_{11}\text{Cl}_2\text{F}_3\text{N}_6\text{O}_3\text{S}$ ,  $[\text{M}]^+$  555.1453 Found 555.1421.

**3.4.3. (E)-2-((4-Chloro-2-((E)-((5-chloropyrazin-2-yl)imino)methyl)phenyl)imino)-3-(3-chloro-4-methylphenyl)thiazolidin-4-one (3).** Yield, 59%; white solid,  $R_f$  value 0.49 (7:3 n-hex: EtOAc) m.p. 194–195°C;  $^1\text{H-NMR}$  (600 MHz, DMSO- $d_6$ ):  $\delta$  9.27 (s, 1H, N=CH), 8.88 (s, 1H, Cl-pyrazin-H), 8.69 (s, 1H, Cl-pyrazin-H), 8.62 (s, Ar-H, 1H), 8.41 (d,  $J$  = 8.4 Hz, Ar-H, 1H), 8.36 (s, Ar-H, 1H), 8.31 (d, 1H, Ar-H,  $J$  = 8.4 Hz), 8.20

TABLE 1: The various substitution patterns of the aromatic ring in the compounds (1-12) along with acetylcholinesterase inhibitory profile.

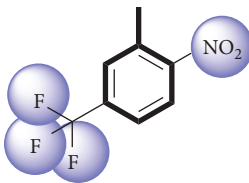
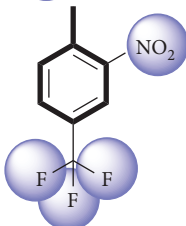
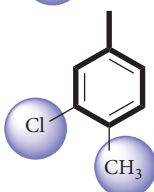
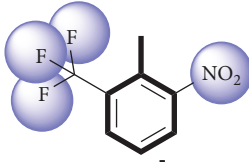
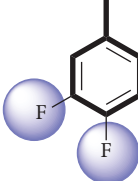
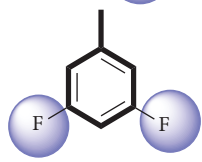
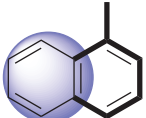
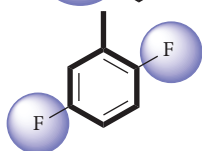
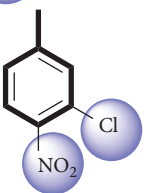
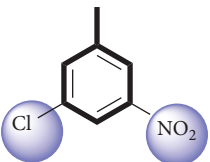
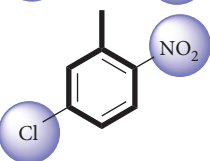
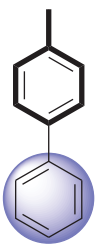
| S/No. | R   | AChE inhibition $IC_{50} \pm SEM$<br>( $\mu M$ ) |
|-------|---|--|
| 1     |    | $4.10 \pm 0.20$                                  |
| 2     |    | $2.20 \pm 0.20$                                  |
| 3     |    | $8.10 \pm 0.10$                                  |
| 4     |   | $2.30 \pm 0.20$                                  |
| 5     |  | $5.80 \pm 0.30$                                  |
| 6     |  | $6.30 \pm 0.20$                                  |
| 7     |  | $19.10 \pm 0.20$                                 |
| 8     |  | $5.20 \pm 0.10$                                  |
| 9     |  | $5.20 \pm 0.40$                                  |

TABLE 1: Continued.

| S/No. | R   | AChE inhibition IC <sub>50</sub> ± SEM (μM) |
|-------|---|---|
| 10    |  | 8.30 ± 0.40                                 |
| 11    |  | 8.10 ± 0.70                                 |
| 12    |  | 20.30 ± 0.30                                |
|       | Standard donepezil drug   | 10.10 ± 0.10 μM                             |

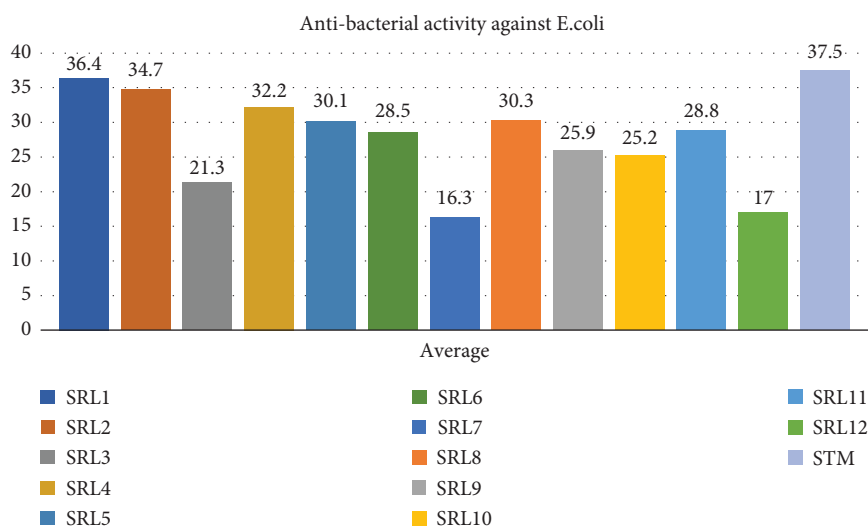


FIGURE 3: The antibacterial profile of synthesized scaffolds (1-12).

(d,  $J = 8.0$  Hz, Ar-H, 1H), 8.04 (d,  $J = 8.3$  Hz, Ar-H, 1H), 3.57 (s, 2H, S-CH<sub>2</sub>), 2.54 (s, 3H, Ar-CH<sub>3</sub>); <sup>13</sup>C-NMR (150 MHz, DMSO-d<sub>6</sub>): δ 183.9, 168.0, 160.7, 159.8, 159.1, 157.6, 155.7, 155.2, 147.9, 141.5, 141.6, 139.7, 134.2, 130.5, 129.1, 119.3, 119.7, 117.4, 114.2, 54.3, 32.9; HREI-MS:  $m/z$  calculated for C<sub>21</sub>H<sub>14</sub>Cl<sub>3</sub>N<sub>5</sub>O<sub>5</sub>, [M]<sup>+</sup> 490.9345 Found 490.9328.

3.4.4. (*E*)-2-((4-Chloro-2-((*E*)-((5-chloropyrazin-2-yl)imino)methyl)phenyl)imino)-3-(2-nitro-6-(trifluoromethyl)phenyl)thiazolidin-4-one (4). Yield, 68%; yellow solid,  $R_f$  value 0.51 (7:3 n-hex: EtOAc) m.p. 189-190°C; <sup>1</sup>H-NMR (600 MHz, DMSO-d<sub>6</sub>): δ 9.21 (s, 1H, N=CH), 8.91 (s, 1H, Cl-pyrazin-H), 8.66 (s, 1H, Cl-pyrazin-H), 8.59 (dd,  $J = 8.6, 1.4$  Hz, Ar-H, 1H), 8.47 (d,  $J = 8.5$  Hz, Ar-H, 1H), 8.33 (s, Ar-H, 1H),

8.29 (dd, Ar-H, 1H,  $J = 8.0, 1.5$  Hz), 8.20 (t,  $J = 8.5$  Hz, Ar-H, 1H), 7.97 (d,  $J = 8.1$  Hz, Ar-H, 1H), 3.54 (s, 2H, S-CH<sub>2</sub>); <sup>13</sup>C-NMR (150 MHz, DMSO-d<sub>6</sub>): δ 186.1, 171.3, 170.1, 157.6, 150.9, 150.2, 148.8, 148.2, 148.7, 148.4, 147.3, 147.2, 142.9, 141.2, 140.5, 137.2, 124.6, 116.4, 114.0, 113.5, 56.8; Found HREI-MS:  $m/z$  calculated for C<sub>21</sub>H<sub>11</sub>Cl<sub>2</sub>F<sub>3</sub>N<sub>6</sub>O<sub>3</sub>S, [M]<sup>+</sup> 555.2387 Found 555.2373.

3.4.5. (*E*)-2-((4-Chloro-2-((*E*)-((5-chloropyrazin-2-yl)imino)methyl)phenyl)imino)-3-(3,4-difluorophenyl)thiazolidin-4-one (5). Yield, 61%; brown solid,  $R_f$  value 0.58 (7:3 n-hex: EtOAc) m.p. 180-181°C; <sup>1</sup>H-NMR (600 MHz, DMSO-d<sub>6</sub>): δ 9.25 (s, 1H, N=CH), 8.92 (s, 1H, Cl-pyrazin-H), 8.73 (s, 1H, Cl-pyrazin-H), 8.68 (s, Ar-H, 1H), 8.52 (d,  $J = 8.7$  Hz, Ar-H,



TABLE 2: Representation of protein-ligand interactions with the docking score and distances for potent compounds **1 (A)**, **2 (B)**, **4 (C)**, and **5 (D)** in the AChE complex.

| Potential analogs                         | Covered distance (Å°)                     | Bonding                | Interactive sites     | Docking score |
|---|---|------------------------|-----------------------|---------------|
| Compound <b>1 (A)</b> in AchE complex     | 6.59                                      | $\pi$ -S               | PHE-A-329             | -11.47        |
|   | 4.85                                      | $\pi$ -R               | ALA-A-238             |               |
|   | 7.04                                      | H-B                    | TYR-A-332             |               |
|   | 5.54                                      | H-B                    | TYR-A-332             |               |
|   | 6.47                                      | $\pi$ - $\pi$ T shaped | TYR-A-332             |               |
|   | 5.01                                      | $\pi$ -R               | TYR-A-332             |               |
|   | 4.50                                      | C-H                    | HIS-A-438             |               |
|   | 6.71                                      | $\pi$ -R               | TRP-A-430             |               |
|   | 6.70                                      | $\pi$ -R               | TRP-A-430             |               |
|   | 3.81                                      | $\pi$ -R               | TRP-A-430             |               |
|   | 5.53                                      | H-F                    | GLY-A-78              |               |
|   | 5.01                                      | $\pi$ -R               | TRP-A-82              |               |
|   | 5.20                                      | C-H                    | TRP-A-82              |               |
| 4.98                                      | C-H                                       | SER-A-287              |                       |               |
| Compound <b>2 (B)</b> in the AchE complex | 4.48                                      | H-F                    | PRO-A-285             | -11.46        |
|   | 5.39                                      | H-F                    | PRO-A-285             |               |
|   | 4.85                                      | $\pi$ -R               | PHE-A-329             |               |
|   | 4.18                                      | C-H                    | HIS-A-438             |               |
|   | 3.91                                      | $\pi$ -S               | TRP-A-82              |               |
|   | 5.15                                      | $\pi$ -R               | VAL-A-288             |               |
|   | 4.48                                      | $\pi$ -R               | LEU-A-286             |               |
|   | 3.78                                      | $\pi$ -Sigma           | TRP-A-231             |               |
|   | 4.45                                      | $\pi$ - $\pi$ T shaped | GLY-A-116             |               |
|   | 6.25                                      | H-B                    | TYR-A-332             |               |
|   | 3.87                                      | $\pi$ -R               | TYR-A-332             |               |
|   | 3.38                                      | $\pi$ -R               | TYR-A-332             |               |
|   | Compound <b>4 (C)</b> in the AchE complex | 3.78                   | $\pi$ - $\pi$ stacked |               |
| 6.55                                      |   | $\pi$ -R               | HIS-A-438             |               |
| 6.75                                      |   | $\pi$ -R               | PHE-A-398             |               |
| 5.78                                      |   | $\pi$ -R               | LEU-A-286             |               |
| 4.22                                      |   | $\pi$ -R               | PHE-A-329             |               |
| 5.77                                      |   | $\pi$ -R               | PHE-A-329             |               |
| 4.25                                      |   | $\pi$ -R               | PHE-A-329             |               |
| 6.60                                      |   | $\pi$ - $\pi$ stacked  | PHE-A-329             |               |
| 5.61                                      |   | H-F                    | ASP-A-70              |               |
| 6.69                                      |   | $\pi$ -R               | ALA-A-328             |               |
| 4.83                                      |   | C-H                    | TRP-A-82              |               |
| 5.34                                      |   | C-H                    | SER-A-287             |               |
| Compound <b>5 (D)</b> in the AchE complex |   | 3.78                   | H-F                   | ASP-A-70      |
|   | 6.11                                      | $\pi$ - $\pi$ T shaped | TRP-A-82              |               |
|   | 6.71                                      | $\pi$ -R               | TRP-A-430             |               |
|   | 5.34                                      | $\pi$ -R               | TRP-A-332             |               |
|   | 3.70                                      | $\pi$ -R               | ALA-A-328             |               |
|   | 6.27                                      | $\pi$ -R               | ALA-A-328             |               |
|   | 5.07                                      | H-B                    | SER-A-198             |               |
|   | 5.52                                      | $\pi$ - $\pi$ T shaped | HIS-A-438             |               |
|   | 5.38                                      | H-B                    | HIS-A-438             |               |
|   | 3.87                                      | $\pi$ -Sigma           | TRP-A-231             |               |
|   | 7.41                                      | $\pi$ - $\pi$ T shaped | TRP-A-231             |               |
|   | 4.98                                      | $\pi$ -R               | VAL-A-288             |               |
|   | 6.21                                      | $\pi$ - $\pi$ T shaped | PHE-A-329             |               |
| 4.13                                      | H-B                                       | THR-A-120              |                       |               |



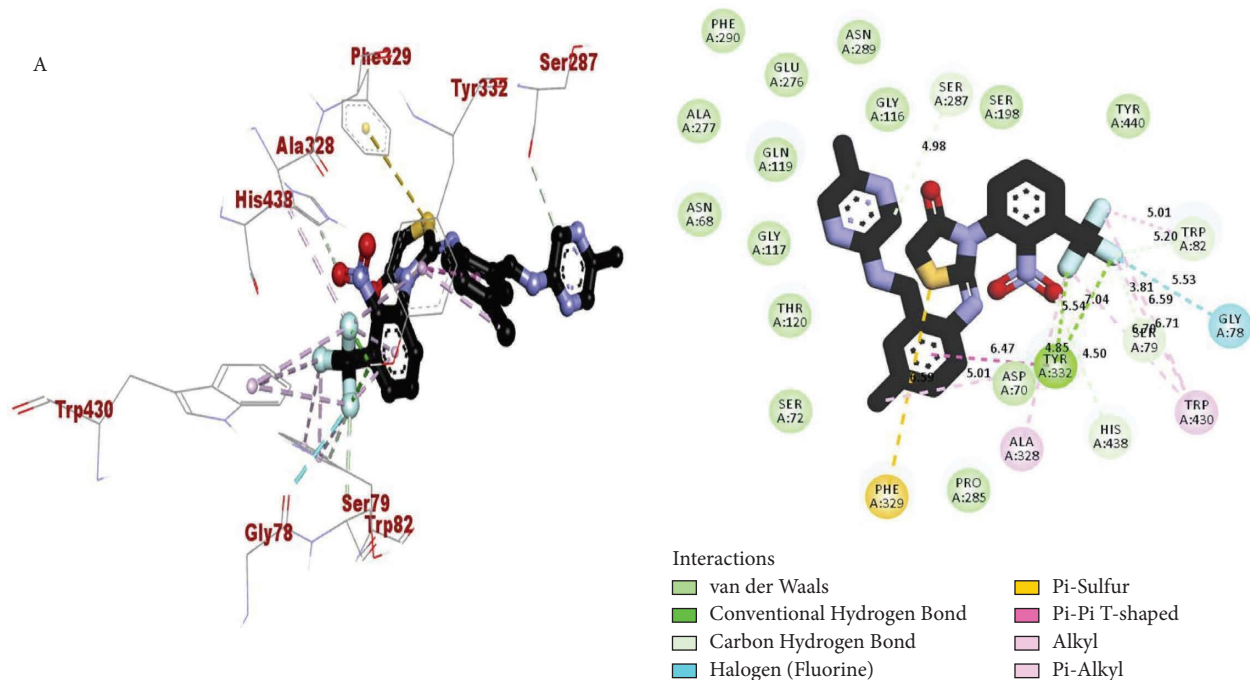


FIGURE 4: 2D/3D representation of analog 1 in the AchE complex.

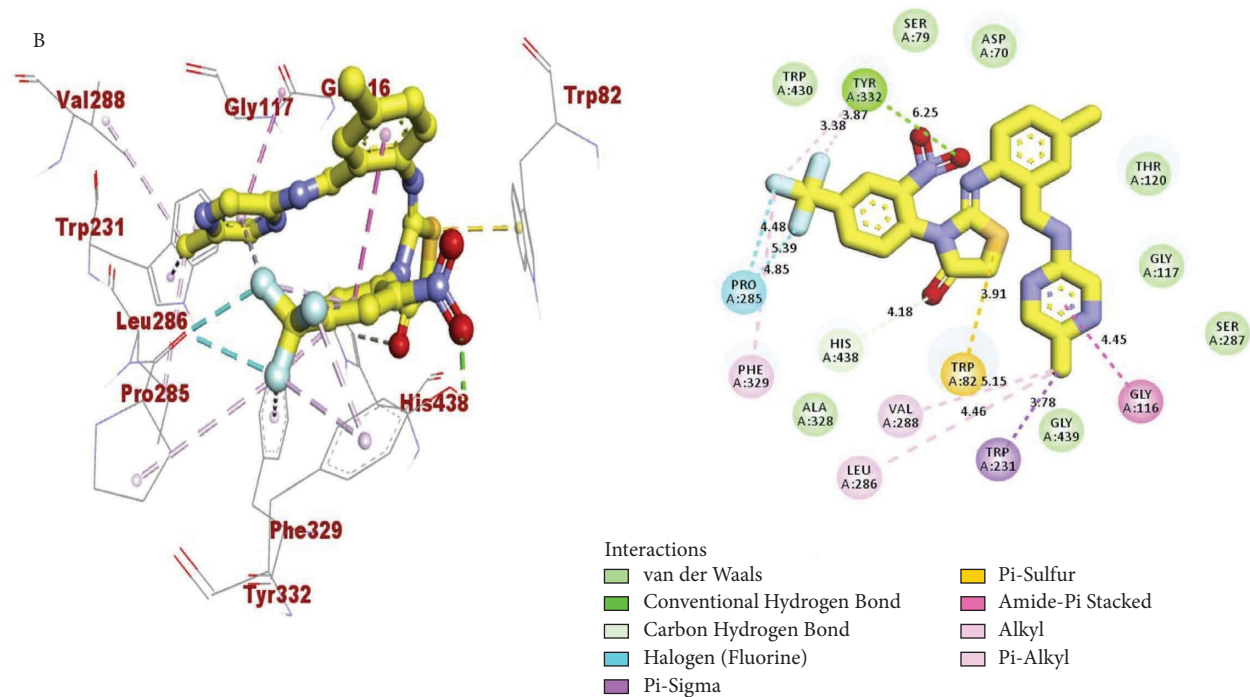


FIGURE 5: 2D/3D representation of analog 2 in the AchE complex.

1H), 8.39 (s, Ar-H, 1H), 8.36 (d, Ar-H, 1H,  $J = 8.5$  Hz), 8.28 (d,  $J = 8.5$  Hz, Ar-H, 1H), 8.09 (d,  $J = 8.8$  Hz, Ar-H, 1H), 3.51 (s, 2H, S-CH<sub>2</sub>); <sup>13</sup>C-NMR (150 MHz, DMSO-d<sub>6</sub>):  $\delta$  187.3, 172.1, 170.8, 162.3, 160.3, 160.1, 155.5, 155.7, 153.1, 146.4, 141.5, 139.4, 133.1, 132.4, 129.8, 124.5, 122.1, 121.7, 120.0, 54.9; HREI-MS:  $m/z$  calculated for C<sub>20</sub>H<sub>11</sub>Cl<sub>2</sub>F<sub>2</sub>N<sub>5</sub>OS, [M]<sup>+</sup> 478.1609 Found 478.1632.

3.4.6. (*E*)-2-((4-Chloro-2-((*E*)-((5-chloropyrazin-2-yl)imino)methyl)phenyl)imino)-3-(3,5-difluorophenyl)thiazolidin-4-one (6). Yield, 66%; white solid,  $R_f$  value 0.59 (7 : 3 n-hex: EtOAc) m.p. 185-186°C; <sup>1</sup>H-NMR (600 MHz, DMSO-d<sub>6</sub>):  $\delta$  9.24 (s, 1H, N=CH), 8.87 (s, 1H, Cl-pyrazin-H), 8.73 (s, 1H, Cl-pyrazin-H), 8.65 (s, Ar-H, 1H), 8.50 (d,  $J = 8.3$  Hz, Ar-H, 1H), 8.40 (s, Ar-H, 1H), 8.31 (d, Ar-H, 1H,  $J = 8.0$  Hz), 8.29



1.6 Hz, 1H, Naph-H), 8.32 (dd, 2H,  $J = 8.0, 1.5$  Hz, Naph-H), 8.24 (dd, 1H,  $J = 8.2, 1.8$  Hz, Naph-H), 8.11 (t,  $J = 8.7$  Hz, 1H, Naph-H), 8.01 (t,  $J = 8.2$  Hz, 2H, Naph-H), 7.87 (d,  $J = 8.0$  Hz, Ar-H, 1H), 7.82 (d,  $J = 8.6$  Hz, Ar-H, 1H), 3.49 (s, 2H, S-CH<sub>2</sub>); <sup>13</sup>C-NMR (150 MHz, DMSO-d<sub>6</sub>):  $\delta$  188.4, 177.8, 176.5, 174.5, 173.5, 170.2, 169.8, 163.5, 163.2, 161.8, 160.9, 160.4, 146.3, 143.2, 139.8, 137.9, 136.5, 136.7, 129.8, 128.9, 118.2, 116.1, 113.1, 55.9; HREI-MS:  $m/z$  calculated for C<sub>24</sub>H<sub>15</sub>Cl<sub>2</sub>N<sub>5</sub>O<sub>5</sub>, [M]<sup>+</sup> 492.9736 Found 492.9711.

3.4.8. (E)-2-((4-Chloro-2-((E)-((5-chloropyrazin-2-yl)imino)methyl)phenyl)imino)-3-(2,5-difluorophenyl)thiazolidin-4-one (8). Yield, 60%; white solid  $R_f$  value 0.53 (7:3 n-hex: EtOAc) m.p. 180-181°C; <sup>1</sup>H-NMR (600 MHz, DMSO-d<sub>6</sub>):  $\delta$  9.17 (s, 1H, N=CH), 8.93 (s, 1H, Cl-pyrazin-H), 8.74 (s, 1H, Cl-pyrazin-H), 8.69 (s, Ar-H, 1H), 8.53 (d,  $J = 9.0$  Hz, Ar-H, 1H), 8.38 (s, Ar-H, 1H), 8.33 (d, Ar-H, 1H,  $J = 8.0$  Hz), 8.25 (d,  $J = 8.9$  Hz, Ar-H, 1H), 8.02 (d,  $J = 8.4$  Hz, Ar-H, 1H), 3.52 (s, 2H, S-CH<sub>2</sub>); <sup>13</sup>C-NMR (150 MHz, DMSO-d<sub>6</sub>):  $\delta$  189.3, 175.4, 173.7, 162.2, 161.2, 160.9, 157.6, 156.2, 155.9, 149.8, 147.5, 138.2, 136.5, 132.8, 129.9, 124.4, 122.6, 122.2, 121.0, 54.9; HREI-MS:  $m/z$  calculated for C<sub>20</sub>H<sub>11</sub>Cl<sub>2</sub>F<sub>2</sub>N<sub>5</sub>O<sub>5</sub>, [M]<sup>+</sup> 478.0854 Found 478.0835.

3.4.9. (E)-2-((4-Chloro-2-((E)-((5-chloropyrazin-2-yl)imino)methyl)phenyl)imino)-3-(3-chloro-4-nitrophenyl)thiazolidin-4-one (9). Yield, 67%; pale green solid,  $R_f$  value 0.48 (7:3 n-hex: EtOAc) m.p. 203-204°C; <sup>1</sup>H-NMR (600 MHz, DMSO-d<sub>6</sub>):  $\delta$  9.18 (s, 1H, N=CH), 8.96 (s, 1H, Cl-pyrazin-H), 8.70 (s, 1H, Cl-pyrazin-H), 8.64 (s, Ar-H, 1H), 8.58 (d,  $J = 8.9$  Hz, Ar-H, 1H), 8.43 (s, Ar-H, 1H), 8.38 (d, 1H, Ar-H,  $J = 8.8$  Hz), 8.29 (d,  $J = 8.7$  Hz, Ar-H, 1H), 8.12 (d,  $J = 8.4$  Hz, Ar-H, 1H), 3.58 (s, 2H, S-CH<sub>2</sub>); <sup>13</sup>C-NMR (150 MHz, DMSO-d<sub>6</sub>):  $\delta$  187.4, 173.1, 172.7, 169.2, 167.2, 163.9, 159.3, 158.2, 158.0, 152.8, 147.4, 139.1, 138.6, 136.7, 131.9, 127.4, 125.6, 124.2, 121.6, 58.0; HREI-MS:  $m/z$  calculated for C<sub>20</sub>H<sub>11</sub>Cl<sub>3</sub>N<sub>6</sub>O<sub>5</sub>S, [M]<sup>+</sup> 521.3214 Found 521.3185.

3.4.10. (E)-2-((4-Chloro-2-((E)-((5-chloropyrazin-2-yl)imino)methyl)phenyl)imino)-3-(3-chloro-5-nitrophenyl)thiazolidin-4-one (10). Yield, 65%; white solid,  $R_f$  value 0.52 (7:3 n-hex: EtOAc) m.p. 208-209°C; <sup>1</sup>H-NMR (600 MHz, DMSO-d<sub>6</sub>):  $\delta$  9.22 (s, 1H, N=CH), 8.81 (s, 1H, Cl-pyrazin-H), 8.79 (s, 1H, Cl-pyrazin-H), 8.69 (s, Ar-H, 1H), 8.56 (d,  $J = 8.4$  Hz, Ar-H, 1H), 8.49 (s, Ar-H, 1H), 8.38 (d, 1H, Ar-H,  $J = 8.6$  Hz), 8.31 (s, Ar-H, 1H), 8.19 (s, Ar-H, 1H), 3.59 (s, 2H, S-CH<sub>2</sub>); <sup>13</sup>C-NMR (150 MHz, DMSO-d<sub>6</sub>):  $\delta$  186.7, 173.8, 172.9, 171.3, 168.2, 167.8, 165.7, 160.9, 156.9, 149.8, 143.6, 141.5, 139.3, 137.8, 129.8, 128.9, 127.2, 119.7, 118.2, 56.1; HREI-MS:  $m/z$  calcd for C<sub>20</sub>H<sub>11</sub>Cl<sub>3</sub>N<sub>6</sub>O<sub>5</sub>S, [M]<sup>+</sup> 521.9851 Found 521.9811.

3.4.11. (E)-2-((4-Chloro-2-((E)-((5-chloropyrazin-2-yl)imino)methyl)phenyl)imino)-3-(5-chloro-2-nitrophenyl)thiazolidin-4-one (11). Yield, 62%; pale white solid,  $R_f$  value 0.54 (7:3 n-hex: EtOAc) m.p. 198-199°C; <sup>1</sup>H-NMR (600 MHz, DMSO-d<sub>6</sub>):  $\delta$  9.18 (s, 1H, N=CH), 8.90 (s, 1H, Cl-pyrazin-H), 8.67

(s, 1H, Cl-pyrazin-H), 8.64 (s, Ar-H, 1H), 8.57 (d, Ar-H,  $J = 9.2$  Hz, 1H), 8.43 (s, Ar-H, 1H), 8.36 (d, Ar-H, 1H,  $J = 8.8$  Hz), 8.31 (d,  $J = 8.2$  Hz, Ar-H, 1H), 8.22 (d,  $J = 8.9$  Hz, Ar-H, 1H), 3.51 (s, 2H, S-CH<sub>2</sub>); <sup>13</sup>C-NMR (150 MHz, DMSO-d<sub>6</sub>):  $\delta$  188.4, 174.7, 172.6, 166.5, 163.5, 150.9, 149.6, 146.2, 145.9, 139.8, 137.5, 133.2, 130.5, 122.8, 122.5, 121.4, 120.6, 120.2, 119.0, 54.9; HREI-MS:  $m/z$  calculated for C<sub>20</sub>H<sub>11</sub>Cl<sub>3</sub>N<sub>6</sub>O<sub>5</sub>S, [M]<sup>+</sup> 521.1259 Found 521.1231.

3.4.12. (E)-3-([1,1'-Biphenyl]-4-yl)-2-((4-chloro-2-((E)-((5-chloropyrazin-2-yl)imino)methyl)phenyl)imino)thiazolidin-4-one (12). Yield, 69%; off-white solid,  $R_f$  value 0.50 (7:3 n-hex: EtOAc) m.p. 218-219°C; <sup>1</sup>H-NMR (600 MHz, DMSO-d<sub>6</sub>):  $\delta$  9.16 (s, 1H, N=CH), 8.84 (s, 1H, Cl-pyrazin-H), 8.76 (s, 1H, Cl-pyrazin-H), 8.69 (s, 1H, Ar-H), 8.59 (d,  $J = 8.4$  Hz, 2H, Biph-H), 8.44 (d, 2H,  $J = 8.2$  Hz, Biph-H), 8.25 (dd, 2H,  $J = 8.8, 2.6$  Hz, Naph-H), 8.17 (t,  $J = 8.7$  Hz, 2H, Naph-H), 8.08 (m,  $J = 8.7$  Hz, 1H, Naph-H), 7.88 (d,  $J = 8.4$  Hz, Ar-H, 1H), 7.80 (d, Ar-H,  $J = 8.0$  Hz, 1H), 3.59 (s, 2H, S-CH<sub>2</sub>); <sup>13</sup>C-NMR (150 MHz, DMSO-d<sub>6</sub>):  $\delta$  181.4, 169.8, 168.5, 165.5, 163.6, 160.0, 159.8, 153.9, 153.7, 151.8, 150.9, 150.4, 146.5, 145.6, 142.4, 139.4, 137.5, 138.7, 134.8, 133.2, 132.5, 116.5, 114.6, 112.9, 112.6, 55.0; HREI-MS:  $m/z$  calculated for C<sub>26</sub>H<sub>17</sub>Cl<sub>2</sub>N<sub>5</sub>O<sub>5</sub>S, [M]<sup>+</sup> 518.9512 Found 518.9481.

## 4. Conclusion

The molecular structures of pyrazine-based thiazolidinone derivatives (1–12) were verified using different characterization methods such as NMR (<sup>1</sup>H and <sup>13</sup>C) and HREI-MS. The therapeutic potential of these derivatives for the treatment of Alzheimer's disease was then assessed by examining their inhibitory effects in comparison to donepezil (IC<sub>50</sub> = 10.10 ± 0.10 μM). Specifically, the compounds **1**, **2**, **4**, **5**, **6**, **8**, **9**, **10**, and **11** exhibited significant activity having IC<sub>50</sub> values of 4.10 ± 0.20, 2.20 ± 0.20, 2.30 ± 0.20, 5.80 ± 0.30, 6.30 ± 0.20, 5.20 ± 0.10, 5.20 ± 0.40, 8.30 ± 0.40, and 8.10 ± 0.70 μM, respectively. Furthermore, the synthesized chemical entities underwent screening to evaluate their effectiveness against *E. coli* bacteria. All of the aforementioned compounds exhibited improved levels of inhibition in comparison to the reference antibiotic agent, streptomycin. Further investigation was undertaken on these synthesized compounds using molecular docking analysis to elucidate their interactions with the active sites of enzymes. Sub-optimal performance was discovered in several compounds, namely, **3**, **7**, and **12**. The diminished biological efficacy of these analogs can be ascribed to the existence of a bulky group attached to these moieties on the aromatic ring.

## Data Availability

The data used to support the findings of this study are confidential.

## Conflicts of Interest

The authors declare that they have no conflicts of interest in this study.

## References

- [1] S. Ahmad, F. Iftikhar, F. Ullah, A. Sadiq, and U. Rashid, "Rational design and synthesis of dihydropyrimidine based dual binding site acetylcholinesterase inhibitors," *Bioorganic Chemistry*, vol. 69, pp. 91–101, 2016.
- [2] D. S. Auld, T. J. Kornecook, S. Bastianetto, and R. Quirion, "Alzheimer's disease and the basal forebrain cholinergic system: relations to  $\beta$ -amyloid peptides, cognition, and treatment strategies," *Progress in Neurobiology*, vol. 68, no. 3, pp. 209–245, 2002.
- [3] R. L. Adams, P. L. Craig, and O. A. Parsons, "Neuropsychology of dementia," *Neurologic Clinics*, vol. 4, no. 2, pp. 387–404, 1986.
- [4] P. S. Aisen and K. L. Davis, "The search for disease-modifying treatment for Alzheimer's disease," *Neurology*, vol. 48, no. 6, pp. 35S–41S, 1997.
- [5] M. W. Jann, "Preclinical pharmacology of metrifonate," *Pharmacotherapy: The Journal of Human Pharmacology and Drug Therapy*, vol. 18, no. 2P2, pp. 55–67, 1998.
- [6] J. Massoulié, L. Pezzementi, S. Bon, E. Krejci, and F. M. Vallette, "Molecular and cellular biology of cholinesterases," *Progress in Neurobiology*, vol. 41, no. 1, pp. 31–91, 1993.
- [7] G. H. Mushtaq, N. A. Greig, J. A. Khan, and M. Kamal, "Status of acetylcholinesterase and butyrylcholinesterase in Alzheimer's disease and type 2 diabetes mellitus," *CNS & Neurological Disorders-Drug Targets*, vol. 13, no. 8, pp. 1432–1439, 2014.
- [8] D. J. Ecobichon and A. M. Comeau, "Pseudocholinesterases of mammalian plasma: physicochemical properties and organophosphate inhibition in eleven species," *Toxicology and Applied Pharmacology*, vol. 24, no. 1, pp. 92–100, 1973.
- [9] F. Rahim, M. T. Javed, H. Ullah et al., "Synthesis, molecular docking, acetylcholinesterase and butyrylcholinesterase inhibitory potential of thiazole analogs as new inhibitors for Alzheimer disease," *Bioorganic Chemistry*, vol. 62, pp. 106–116, 2015.
- [10] F. Rahim, H. Ullah, M. Taha et al., "Synthesis and in vitro acetylcholinesterase and butyrylcholinesterase inhibitory potential of hydrazide based Schiff bases," *Bioorganic Chemistry*, vol. 68, pp. 30–40, 2016.
- [11] A. Cavalli, M. L. Bolognesi, A. Minarini et al., "Multi-target-directed ligands to combat neurodegenerative diseases," *Journal of Medicinal Chemistry*, vol. 51, no. 3, pp. 347–372, 2008.
- [12] K. Rockwood, J. Mintzer, L. Truyen, T. Wessel, and D. Wilkinson, "Effects of a flexible galantamine dose in Alzheimer's disease: a randomised, controlled trial," *Journal of Neurology, Neurosurgery & Psychiatry*, vol. 71, no. 5, pp. 589–595, 2001.
- [13] M. Mesulam, A. Guillozet, P. Shaw, and B. Quinn, "Widely spread butyrylcholinesterase can hydrolyze acetylcholine in the normal and Alzheimer brain," *Neurobiology of Disease*, vol. 9, no. 1, pp. 88–93, 2002.
- [14] N. H. Greig, T. Utsuki, Q. S. Yu et al., "A new therapeutic target in Alzheimer's disease treatment: attention to butyrylcholinesterase," *Current Medical Research and Opinion*, vol. 17, no. 3, pp. 159–165, 2001.
- [15] M. T. Gabr and M. S. Abdel-Raziq, "Design and synthesis of donepezil analogues as dual AChE and BACE-1 inhibitors," *Bioorganic Chemistry*, vol. 80, pp. 245–252, 2018.
- [16] D. Melzer, "Personal paper: new drug treatment for Alzheimer's disease: lessons for healthcare policy," *BMJ*, vol. 316, no. 7133, pp. 762–764, 1998.
- [17] H. C. Beck, A. M. Hansen, and F. R. Lauritsen, "Novel pyrazine metabolites found in polymyxin biosynthesis by *Paenibacillus polymyxa*," *FEMS Microbiology Letters*, vol. 220, no. 1, pp. 67–73, 2003.
- [18] M. Kucerova-Chlupacova, J. Kunes, V. Buchta, M. Vejsova, and V. Opletalova, "Novel pyrazine analogs of chalcones: synthesis and evaluation of their antifungal and antimycobacterial activity," *Molecules*, vol. 20, no. 1, pp. 1104–1117, 2015.
- [19] R. Müller and S. Rappert, "Pyrazines: occurrence, formation and biodegradation," *Applied Microbiology and Biotechnology*, vol. 85, no. 5, pp. 1315–1320, 2010.
- [20] J. S. Dickschat, S. Wickel, C. J. Bolten, T. Nawrath, S. Schulz, and C. Wittmann, "Pyrazine biosynthesis in *Corynebacterium glutamicum*," *European Journal of Organic Chemistry*, vol. 2010, pp. 2687–2695, 2010.
- [21] K. S. Rajini, P. Aparna, C. Sasikala, and C. V. Ramana, "Microbial metabolism of pyrazines," *Critical Reviews in Microbiology*, vol. 37, no. 2, pp. 99–112, 2011.
- [22] D. Rybakova, T. Cernava, M. Köberl, S. Liebminger, M. Etemadi, and G. Berg, "Endophytes-assisted biocontrol: novel insights in ecology and the mode of action of *Paenibacillus*," *Plant and Soil*, vol. 405, no. 1–2, pp. 125–140, 2016.
- [23] X. Lian, S. Wang, G. Xu, N. Lin, Q. Li, and H. Zhu, "The application with tetramethyl pyrazine for antithrombogenicity improvement on silk fibroin surface," *Applied Surface Science*, vol. 255, no. 2, pp. 480–482, 2008.
- [24] B. A. Milczarska, H. E. Foks, J. Sokołowska, M. I. Janowiec, Z. Zwolska, and Z. Andrzejczyk, "Studies on pyrazine derivatives. XXXIII. Synthesis and tuberculostatic activity of 1-[1-(2-pyrazinyl)-ethyl]-4-N-substituted thiosemicarbazide derivatives," *Acta Poloniae Pharmaceutica*, vol. 56, no. 2, pp. 121–126, 1999.
- [25] A. Hameed, S. T. Zehra, S. J. A. Shah et al., "Syntheses, cholinesterases inhibition, and molecular docking studies of pyrido[2,3-b]pyrazine derivatives," *Chemical Biology & Drug Design*, vol. 86, no. 5, pp. 1115–1120, 2015.
- [26] M. Taha, N. H. Ismail, S. Imran et al., "In silico binding analysis and SAR elucidations of newly designed benzopyrazine analogs as potent inhibitors of thymidine phosphorylase," *Bioorganic Chemistry*, vol. 68, pp. 80–89, 2016.
- [27] Y. J. Surh, S. G. Kim, K. K. Park et al., "Chemopreventive effects of 2-(allylthio) pyrazine on hepatic lesion, mutagenesis and tumorigenesis induced by vinyl carbamate or vinyl carbamate epoxide," *Carcinogenesis*, vol. 19, no. 7, pp. 1263–1267, 1998.
- [28] S. G. Kim, G. L. Kedderis, R. Batra, and R. F. Novak, "Induction of rat liver microsomal epoxide hydrolase by thiazole and pyrazine: hydrolysis of 2-cyanoethylene oxide," *Carcinogenesis*, vol. 14, no. 8, pp. 1665–1670, 1993.
- [29] R. Václavíková, D. J. Hughes, and P. Souček, "Microsomal epoxide hydrolase 1 (EPHX1): gene, structure, function, and role in human disease," *Gene*, vol. 571, no. 1, pp. 1–8, 2015.
- [30] C. G. Bonde and N. J. Gaikwad, "Synthesis and preliminary evaluation of some pyrazine containing thiazolines and thiazolidinones as antimicrobial agents," *Bioorganic & Medicinal Chemistry*, vol. 12, no. 9, pp. 2151–2161, 2004.
- [31] T. S. Chitre, K. D. Asgaonkar, P. B. Miniyaar et al., "Synthesis and docking studies of pyrazine-thiazolidinone hybrid scaffold targeting dormant tuberculosis," *Bioorganic & Medicinal Chemistry Letters*, vol. 26, no. 9, pp. 2224–2228, 2016.

- [32] V. Ravichandran, B. Prashantha Kumar, S. Sankar, and R. K. Agrawal, "Predicting anti-HIV activity of 1,3,4-thiazolidinone derivatives: 3D-QSAR approach," *European Journal of Medicinal Chemistry*, vol. 44, no. 3, pp. 1180–1187, 2009.
- [33] R. Suryawanshi, S. Jadhav, N. Makwana et al., "Evaluation of 4-thiazolidinone derivatives as potential reverse transcriptase inhibitors against HIV-1 drug resistant strains," *Bioorganic Chemistry*, vol. 71, pp. 211–218, 2017.
- [34] Y. Tian, P. Zhan, D. Rai, J. Zhang, E. De Clercq, and X. Liu, "Recent advances in the research of 2,3-Diaryl-1,3-thiazolidin-4-one derivatives as potent HIV-1 non-nucleoside reverse transcriptase inhibitors," *Current Medicinal Chemistry*, vol. 19, no. 13, pp. 2026–2037, 2012.
- [35] R. D. Dighe, S. S. Rohom, P. D. Dighe, and M. R. Shiradkar, "Condensed bridgehead nitrogen heterocyclic systems: synthesis and evaluation of isatinyl thiazole derivatives as anti-Mycobacterium tuberculosis agents and dTDP-rhamnose inhibitors," *Der Pharma Chemica*, vol. 3, pp. 418–432, 2011.
- [36] F. Rahim, K. Zaman, H. Ullah et al., "Synthesis of 4-thiazolidinone analogs as potent in vitro anti-urease agents," *Bioorganic Chemistry*, vol. 63, pp. 123–131, 2015.
- [37] A. Ramalingam, S. Sambandam, M. Medimagh, O. Al-Dosary, N. Issaoui, and M. J. Wojcik, "Study of a new piperidone as an anti-Alzheimer agent: molecular docking, electronic and intermolecular interaction investigations by DFT method," *Journal of King Saud University Science*, vol. 33, no. 8, 2021.
- [38] A. Ramalingam, A. R. Guerroudj, S. Sambandam et al., "Synthesis, vibrational spectra, Hirshfeld surface analysis, DFT calculations, and in silico ADMET study of 3-(2-chloroethyl)-2, 6-bis (4-fluorophenyl) piperidin-4-one: a potent anti-Alzheimer agent," *Journal of Molecular Structure*, vol. 1269, Article ID 133845, 2022.
- [39] A. Ramalingam, N. Mustafa, W. J. Chng, M. Medimagh, S. Sambandam, and N. Issaoui, "3-Chloro-3-methyl-2, 6-diarylpiperidin-4-ones as anti-cancer agents: synthesis, biological evaluation, molecular docking, and in silico ADMET prediction," *Biomolecules*, vol. 12, no. 8, p. 1093, 2022.
- [40] Y. Khan, S. Khan, R. Hussain et al., "The synthesis, in vitro bio-evaluation, and in silico molecular docking studies of pyrazoline-thiazole hybrid analogues as promising anti- $\alpha$ -glucosidase and anti-urease agents," *Pharmaceuticals*, vol. 16, no. 12, p. 1650, 2023.
- [41] S. Khan, H. Ullah, R. Hussain et al., "Synthesis, in vitro bio-evaluation, and molecular docking study of thiosemicarbazone-based isatin/bis-schiff base hybrid analogues as effective cholinesterase inhibitors," *Journal of Molecular Structure*, vol. 1284, Article ID 135351, 2023.
- [42] S. Khan, W. Rehman, F. Rahim et al., "Bis-indole based triazine derivatives: synthesis, characterization, in vitro  $\beta$ -glucuronidase anti-cancer and anti-bacterial evaluation along with in silico molecular docking and ADME analysis," *Arabian Journal of Chemistry*, vol. 16, no. 8, Article ID 104970, 2023.
- [43] B. Adalat, F. Rahim, W. Rehman et al., "Biologically potent benzimidazole-based-substituted benzaldehyde derivatives as potent inhibitors for alzheimer's disease along with molecular docking study," *Pharmaceuticals*, vol. 16, no. 2, p. 208, 2023.
- [44] Y. Khan, W. Rehman, R. Hussain et al., "New biologically potent benzimidazole based triazole derivatives as acetylcholinesterase and butyrylcholinesterase inhibitors along with molecular docking study," *Journal of Heterocyclic Chemistry*, vol. 59, no. 12, pp. 2225–2239, 2022.
- [45] S. Khan, H. Ullah, F. Rahim et al., "New thiazole-based thiazolidinone derivatives: synthesis, in vitro  $\alpha$ -amylase,  $\alpha$ -glucosidase activities and silico molecular docking study," *Chemical Data Collections*, vol. 42, Article ID 100967, 2022.
- [46] T. Arumugam, A. Ramalingam, A. R. Guerroudj, S. Sambandam, N. Boukabcha, and A. Chouaih, "Conformation and vibrational spectroscopic analysis of 2, 6-bis (4-fluorophenyl)-3, 3-dimethylpiperidin-4-one (BFDP) by DFT method: a potent anti-Parkinson's, anti-lung cancer, and anti-human infectious agent," *Heliyon*, vol. 9, no. 11, p. e21410, 2023.
- [47] R. Arulraj, S. Sivakumar, S. Suresh, and K. Anitha, "Synthesis, vibrational spectra, DFT calculations, Hirshfeld surface analysis and molecular docking study of 3-chloro-3-methyl-2, 6-diphenylpiperidin-4-one," *Spectrochimica Acta Part A: Molecular and Biomolecular Spectroscopy*, vol. 232, Article ID 118166, 2020.
- [48] A. Ramalingam, M. Kuppusamy, S. Sambandam et al., "Synthesis, spectroscopic, topological, hirshfeld surface analysis, and anti-covid-19 molecular docking investigation of isopropyl 1-benzoyl-4-(benzoyloxy)-2, 6-diphenyl-1, 2, 5, 6-tetrahydropyridine-3-carboxylate," *Heliyon*, vol. 8, no. 10, p. e10910, 2022.
- [49] A. Ramalingam, C. Duraisamy, H. Louis et al., "Study of new carbonitrile as an anti-muscular dystrophy agent: crystal, vibrational spectroscopy, molecular docking, electronic and intermolecular interaction investigations by the DFT method," *Journal of Molecular Structure*, vol. 1299, Article ID 137031, 2024.
- [50] C. Isarankura-Na-Ayudhya, T. Naenna, C. Nantasenam, and V. Prachayasittikul, "A Practical Overview of Quantitative Structure-Activity Relationship," *EXCLI Journal*, vol. 8, pp. 1–10, 2009.
- [51] C. Hansch, "Quantitative approach to biochemical structure-activity relationships," *Accounts of Chemical Research*, vol. 2, no. 8, pp. 232–239, 1969.
- [52] F. Farhadi, B. Khameneh, M. Iranshahi, and M. Iranshahi, "Antibacterial activity of flavonoids and their structure-activity relationship: an update review," *Phytotherapy Research*, vol. 33, no. 1, pp. 13–40, 2019.